Phosphinidene-Bridged MoMn Derivatives of the Thiophosphinidene Complex [$Mo_2Cp_2(\mu$-κ^2:κ^1,η^6-SPMes*)$(CO)_2$] (Mes* = 2,4,6-$C_6H_2{}^tBu_3$)

Belén Alvarez, M. Angeles Alvarez, M. Esther García, Daniel García-Vivó,* and Miguel A. Ruiz*

Departamento de Química Orgánica e Inorgánica/IUQOEM, Universidad de Oviedo, E-33071 Oviedo, Spain.

Abstract

The title complex (**1**) reacted with [$Mn_2(CO)_{10}$] under visible-UV irradiation (toluene solution and quartz glassware) to give a mixture of the phosphinidene complex [MnMoCp(μ-κ^1:κ^1,η^6-PMes*)$(CO)_4$], the cluster [$Mn_2Mo_2Cp_2(\mu$-κ^1:κ^1,η^6-PMes*)(μ_3-S)$(CO)_8$] and the thiophosphinidene complex [MnMoCp(μ-κ^2:κ^1,η^4-SPMes*)$(CO)_5$], in yields of ca. 60, 20 and 10% respectively (Mes* = 2,4,6-$C_6H_2{}^tBu_3$). The major product follows from formal replacement of the $SMoCp(CO)_2$ fragment in **1** with a $Mn(CO)_4$ fragment, and displayed multiple bonding to phosphorus (Mn–P = 2.1414(8) Å); the tetranuclear cluster results from formal insertion of a $Mn_2(CO)_6$ fragment in **1**, with cleavage of P–S and P–Mo bonds, to render a μ_3-S bridged Mn_2Mo core bearing an exocyclic phosphinidene ligand involved in multiple bonding to one of the Mn atoms (Mn–P = 2.140(2) Å); the thiophosphinidene complex (Mn–P = 2.294(1) Å) formally results from addition of sulfur and carbon monoxide to the major MnMo product, a transformation which actually could be performed stepwise, *via* the MnMo thiophosphinidene complex [MnMoCp(μ-κ^2:κ^1,η^6-SPMes*)$(CO)_4$]. When the photolysis of **1** and [$Mn_2(CO)_{10}$] was performed in tetrahydrofuran solution and using conventional glassware, then the V-shaped cluster [$Mn_2MoCp\{\mu$-κ^1:κ^1,η^5-P($C_6H_3{}^tBu_3$)$\}(CO)_8$] was obtained selectively (Mo–Mn = 3.2910(5) Å, Mn–Mn = 2.9223(5) Å), which unexpectedly displays a cyclohexadienylidene-phosphinidene ligand resulting from H-atom abstraction at the aryl ring of the precursor. Density Functional Theory calculations on the complexes [$L_nM(\mu$-κ^1:κ^1,η^6-PMes*)MoCp] (ML_n = $MoCp(CO)_2$, $Mn(CO)_4$, $Co(CO)_3$) revealed that the degree of delocalization of the metal-phosphorus π-bonding interaction over the Mo–P–M chain is significantly conditioned by the heterometal fragment ML_n, it being increased in the order Mn ≤ Mo < Co.

Introduction

Transition-metal complexes with P-donor ligands displaying metal–phosphorus multiple bonding usually are highly reactive towards many different molecules under mild conditions, whereby new molecules with novel geometries and organophosphorus ligands can be synthesized.[1] Among this sort of species, extensive research has been carried out on mononuclear phosphinidene complexes, particularly on those displaying bent geometries (**B** and **C** in Chart 1).[2] Phosphinidene-bridged binuclear complexes, on the other side, also display M–P multiple bonding and coordinative unsaturation around the P atom in their trigonal coordination modes (**D** and **E** in Chart 1), therefore being quite reactive too, and this has enabled the development of a wide chemistry around them.[3] Most of the binuclear complexes reported so far, however, are homometallic species (M = M´), and only a few heterometallic compounds have been described. Carty and co-workers reported the formation of several MoM complexes of type **D** *via* reaction of chlorophosphanyl Mo precursors with the pertinent carbonyl dimers $[M_2(CO)_{2n}]$ (M = Co, Mn),[4] and a few unymmetrical complexes of type **E** were reported by Lang (MnFe),[5] and Malisch (WFe),[6] by starting from suitable mononuclear phosphanyl complexes.

Chart 1. Coordination Modes of Phosphinidene Ligands at Mononuclear and Binuclear Metal Complexes

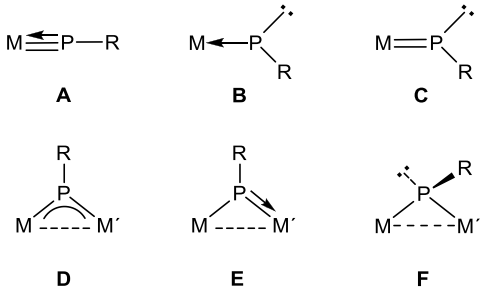

Recently we found that the dimolybdenum complex $[Mo_2Cp_2(\mu\text{-}\kappa^2\text{:}\kappa^1,\eta^6\text{-}SPMes^*)(CO)_2]$ (**1**) (Mes* = 2,4,6-$C_6H_2{}^tBu_3$), a molecule having a rare polyfunctional arylthiophosphinidene ligand (Scheme 1), undergoes easy P–S bond cleavage when reacting with different metal carbonyls, to render phosphinidene ligands bridging different metal atoms and displaying M–P multiple bonding.[7] The reactions with $[W(CO)_6]$ and $[Fe_2(CO)_9]$, which are precursors of 16-electron $M(CO)_x$ fragments, eventually led to $MoM_2(\mu_3\text{-}S)$ clusters bearing exocyclic phosphinidene ligands displaying heterometallic $M(\mu\text{-}\kappa^1\text{:}\kappa^1,\eta^6\text{-}PMes^*)Mo$ connections of type **E**.[7] In contrast, reactions of **1** with $[Co_2(CO)_8]$, a precursor of 17-electron $Co(CO)_4$ fragments, were more complex and could result in full removal of the $SMoCp(CO)_2$ fragment in **1** to yield heterometallic phosphinidene derivatives such as $[CoMoCp(\mu\text{-}\kappa^1\text{:}\kappa^1,\eta^6\text{-}PMes^*)(CO)_3]$ (type **E**), thus effectively accomplishing a transmetallation of the

phosphinidene ligand.[8] It was thus of interest to further explore this sort of reactions in order to prepare novel heterometallic complexes displaying multiple bonding between phosphorus and other transition metal atoms. In this paper we report our results on the photochemical reactions of **1** with $[Mn_2(CO)_{10}]$. Under irradiation with visible-UV light, the manganese dimer is well known to undergo homolytic cleavage of the Mn–Mn bond to yield mononuclear 17-electron $Mn(CO)_5$ radicals, among other photoproducts.[9] Thus, a connection between these photochemical reactions and the dark reactions of **1** with $[Co_2(CO)_8]$ might be found. As it will be shown below, this is indeed the case, and several products involving multiple bonds between P and Mn atoms have been obtained in these reactions. In addition, the nature of these bonding interactions has been analyzed both in the light of Density Functional Theory (DFT) calculations and through some chemical experiments.

Scheme 1. Phosphinidene-Transfer Reactions of Compound 1[a]

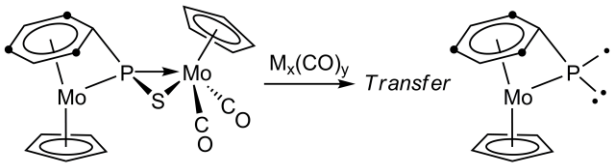

1

[a] M = W, Fe, Co; ● = C–^{t}Bu;

Results and Discussion

Photochemical Reactions of 1 with $[Mn_2(CO)_{10}]$. The results of these reactions were quite sensitive to experimental conditions, particularly the solvent and type of glassware used (quartz or conventional Pyrex glassware). When carried out in toluene solution, quartz glassware had to be used in order to complete the reaction in a reasonable time, but then the selectivity was not very high. Under these conditions, a mixture was formed of the phosphinidene complex $[MnMoCp(\mu\text{-}\kappa^1\text{:}\kappa^1,\eta^6\text{-}PMes^*)(CO)_4]$ (**2**), the thiophosphinidene $[MnMoCp(\mu\text{-}\kappa^2\text{:}\kappa^1,\eta^4\text{-}SPMes^*)(CO)_5]$ (**3**) and the cluster $[Mn_2Mo_2Cp_2(\mu\text{-}\kappa^1\text{:}\kappa^1,\eta^6\text{-}PMes^*)(\mu_3\text{-}S)(CO)_8]$ (**4**), which could be isolated respectively in yields of ca. 60, 10 and 20% after chromatographic workup (Chart 2). Complex **2** follows from formal replacement of the $SMoCp(CO)_2$ fragment in **1** with a $Mn(CO)_4$ fragment, and then is analogous to the mentioned MoCo complex formed in the dark reactions of **1** with $[Co_2(CO)_8]$, while the minor product **3** might be formed upon addition of sulfur and CO to product **2** during reaction, a matter to be discussed below. On the other hand, cluster **4** might be viewed as resulting from formal insertion of a $Mn_2(CO)_6$ fragment in complex **1**, with full cleavage of P–S and P–Mo bonds, to yield a μ_3-S bridged Mn_2Mo cluster bearing an exocyclic phosphinidene ligand bound to one of the Mn atoms; this cluster can be thus related to the products

eventually formed in the reactions of **1** with $[W(CO)_6]$ or $[Fe_2(CO)_9]$, which result in the incorporation of isoelectronic $W_2(CO)_7$ and $Fe_2(CO)_5$ fragments, respectively.[7] We should stress that the presence of the thiophosphinidene ligand at the starting complex **1** is critical to the formation of all these heterometallic products, since a separate experiment revealed that the related phosphinidene complex $[Mo_2Cp_2(\mu\text{-}\kappa^1\text{:}\kappa^1,\eta^6\text{-}PMes^*)(CO)_2]$ (which actually is the synthetic precursor of **1**) failed to react with $[Mn_2(CO)_{10}]$ under analogous photolytic conditions.

In contrast to the above results, the use of tetrahydrofuran as solvent in this photochemical reaction increased the rate enough to be completed in a reasonable time using conventional Pyrex glassware. The reaction was more selective under these conditions since it yielded a single product, but this was identified as the new V-shaped $MoMn_2$ cluster $[Mn_2MoCp\{\mu\text{-}\kappa^1\text{:}\kappa^1\text{:}\kappa^1,\eta^5\text{-}P(C_6H_3{}^tBu_3)\}(CO)_8]$ (**5**), which unexpectedly displays a cyclohexadienylidene-phosphinidene ligand resulting from H-atom abstraction at the aryl ring of the precursor (Chart 2). The formation of **5** can be viewed as resulting from addition of a second odd-electron $Mn(CO)_4$ fragment to the MoMn product **2**. This would give a paramagnetic intermediate rapidly evolving *via* H-atom abstraction (either from the solvent or from traces of water there present) to render the diamagnetic species eventually isolated. Such atom abstraction is a process likely to proceed first at the metal site,[10] then being followed by an H-shift to the aryl group, thus explaining the *endo* positioning of the added H atom in the final cyclohexadienylidene fragment of compound **5**.

Chart 2. Photoproducts of the Reaction of 1 with $[Mn_2(CO)_{10}]$

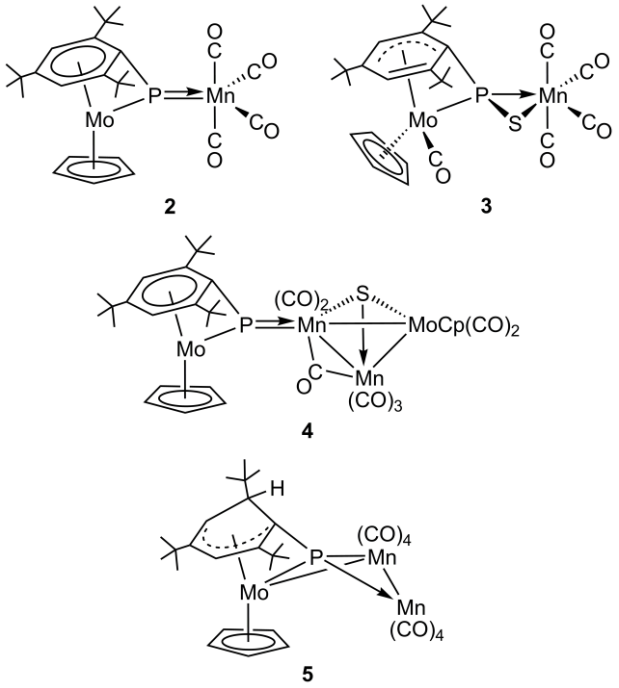

Sulfur Addition to the Phosphinidene Complex 2. As noted above, the structure of the thiophosphinidene complex **3** can be viewed as resulting from addition of sulfur and carbon monoxide to the phosphinidene complex **2**. A separate experiment indicated that this process actually takes place readily at room temperature, thus reproducing the analogous reactivity of the dimolybdenum complex $[Mo_2Cp_2(\mu\text{-}\kappa^1\text{:}\kappa^1,\eta^6\text{-}PMes^*)(CO)_2]$.[11] Indeed, reaction of **2** with S_8 in dichloromethane solution under a CO atmosphere yielded **3** as the unique product (Scheme 2). Moreover, this reaction could be performed stepwise. Thus, compound **2** reacts at room temperature with S_8 to give the thiophosphinidene MoMn complex $[MnMoCp(\mu\text{-}\kappa^2\text{:}\kappa^1,\eta^6\text{-}SPMes^*)(CO)_4]$ (**6**), in a process involving the addition of a sulfur atom to the P–Mn multiple bond of **2** perpendicular to the MoPMn plane, as required for optimum orbital overlap, thus reproducing the behavior of several related dimolybdenum phosphinidene complexes of type **E**.[11] Expectedly, the thiophosphinidene complex **6** rapidly adds a carbonyl under a CO atmosphere to yield **3** selectively, with this involving a η^6 to η^4 slippage of the Mo-bound aryl ring, then reproducing the well-known behavior of the phosphinidene complex $[Mo_2Cp_2(\mu\text{-}\kappa^1\text{:}\kappa^1,\eta^6\text{-}PMes^*)(CO)_2]$.[12] Interestingly, complex **3** could be also obtained selectively through the photochemical reaction (toluene solution, conventional Pyrex glassware) of the thiophosphinidene Mo_2 complex $[Mo_2Cp_2(\mu\text{-}\kappa^2\text{:}\kappa^1,\eta^4\text{-}SPMes^*)(CO)_3]$[11] with $[Mn_2(CO)_{10}]$ (Scheme 2), with no change in the hapticity of the aryl group along the process. This suggests that desulfurization is not a pre-requisite for an effective transmetallation in these complexes, and moreover indicates that these thiophosphinidene complexes may behave not only as transfer reagents of phosphinidene, but also of thiophosphinidene ligands.

Scheme 2. Thiophosphinidene Derivatives of Complex 2[a]

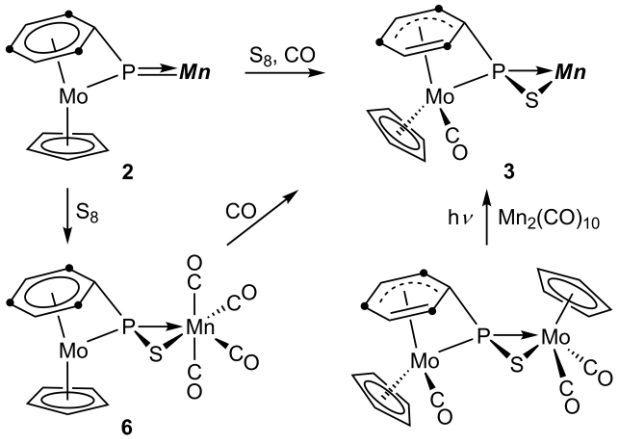

[a] ***Mn*** = $Mn(CO)_4$; ● = C–^{t}Bu

Structure of the Phosphinidene Complex 2. The molecule of the MoMn complex **2** in the crystal (Figure 1 and Table 1) is built up from MoCp and $Mn(CO)_4$ fragments connected through the P atom of the aryl phosphinidene ligand, which in turn completes

the coordination environment of the Mo fragment *via* η^6-binding of the aryl ring. The *ipso* carbon of the latter is located in the MoPMn plane, which in turn roughly bisects the molecule, thus defining a distorted trigonal environment around phosphorus. The overall structure of **2** is thus related to those previously determined for the isoelectronic complexes $[Mo_2Cp_2(\mu\text{-}\kappa^1\text{:}\kappa^1,\eta^6\text{-PMes*})(CO)_2]$[12] and $[CoMoCp(\mu\text{-}\kappa^1\text{:}\kappa^1,\eta^6\text{-PMes*})(CO)_3]$,[7,8] which bear the same 10-electron donor arylphosphinidene ligand. In these compounds, and also in related Mo_2 complexes of type **E** previously studied by us,[13,14] we have generally found M–P distances of magnitude intermediate between the reference values for the corresponding single and double bonds, thus indicating substantial delocalization of the π-bonding interaction along the Mo–P–M chain, facilitated by the geometrical restrictions imposed by bifunctional ligands such as PMes* and PC_5H_4. In the absence of such a restriction, the metallocene Mo fragment tends to rotate away from the phosphinidene plane for steric reasons, thus precluding such a delocalization, with this resulting in the localized interaction depicted for complexes of type **E** in Chart 1, implying M–P bond orders of 1 and 2, respectively. This is the case, for instance, of the PMe-bridged complex $[Mo_2Cp_2(\mu\text{-PMe})(CO)_2(\eta^6\text{-HMes*})]$, which displays very dissimilar Mo–P lengths of 2.538(1) and 2.264(1) Å consistent with their formulation as single and double bonds, respectively.[14] In this context, we might anticipate that the geometry of **2** would allow for the mentioned delocalization along the Mo–P–Mn chain, and indeed the Mo–P length of 2.3704(9) Å falls between the above extreme values, it being only marginally longer than the corresponding length in the Mo_2 complex $[Mo_2Cp_2(\mu\text{-}\kappa^1\text{:}\kappa^1,\eta^6\text{-PMes*})(CO)_2]$ (2.3630(6) Å), but definitely higher than the one in the MoCo complex $[CoMoCp(\mu\text{-}\kappa^1\text{:}\kappa^1,\eta^6\text{-PMes*})(CO)_3]$ (2.326(1) Å). These observations suggest that, in addition to the orientation of the metallocene fragment with respect to the phosphinidene plane, the nature of the heterometal in these arylphosphinidene complexes has a significant influence on the degree of delocalization of the π-bonding interaction along the Mo–P–M chain, a matter to be further analyzed with the help of DFT calculations discussed below. Further indication of π-bonding delocalization along the Mo–P–Mn chain in **2** is given by the Mn–P length of 2.1414(8) Å, which is somewhat longer than the value of 2.084(3) Å measured in the phosphanyl complex $[Mn\{P(OMes*)Cp*\}(CO)_4]$,[15] (a figure taken here as a reference for a double Mn–P bond), but essentially identical to the values of ca. 2.14 Å measured in the Mn_2 compound $[Mn_2\{\mu\text{-}P(N^iPr_2)\}(CO)_6]$,[16] a complex of type **D** for which Mn–P bond orders of 1.5 should be formulated. Interestingly, the FeMn complex $[FeMnCp*\{\mu\text{-}P(OMes*)\}(CO)_6]$ (which incidentally is the only other Mn-containing complex of type **E** structurally characterized so far), displays a Mn–P length of 2.126(2) Å,[6] which

suggests the presence of some (even if reduced) π-bonding delocalization along the Fe–P–Mn chain also in that case.

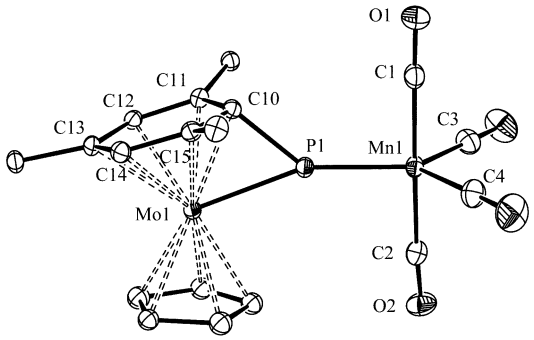

Figure 1. ORTEP diagram (30% probability) of compound **2**, with H atoms and ^{t}Bu groups (except their C^1 atoms) omitted for clarity.

Table 1. Selected Bond Lengths (Å) and Angles (º) for Compound **2**

Mo1–P1	2.3704(9)	Mo1–P1–Mn1	158.99(4)
Mn1–P1	2.1414(8)	Mo1–P1–C10	61.23(8)
Mo1–C10	2.190(3)	Mn1–P1–C10	139.77(9)
Mo1–C11	2.321(3)	P1–Mn1–C1	89.2(1)
Mo1–C12	2.307(3)	P1–Mn1–C2	92.0(1)
Mo1–C13	2.334(3)	P1–Mn1–C3	129.6(1)
Mo1–C14	2.298(3)	P1–Mn1–C4	124.5(1)
Mo1–C15	2.307(3)	C3–Mn1–C4	106.0(2)
P1–C10	1.832(3)	C1–Mn1–C2	176.6(2)

Spectroscopic data in solution for compound **2** (Table 2 and Experimental Section) are consistent with the structure found in the crystal. The phosphinidene ligand gives rise to a quite deshielded resonance (δ_P 522.5 ppm) comparable to those measured in the mentioned Mo_2 (509.7 ppm) and MoCo (627.8 ppm) analogues, as expected from is trigonal environment,[2] and the retention in solution of the η^6 coordination of the aryl ring to the Mo atom is indicated by the equivalence and moderate shielding of the CH groups of this ring (δ_H 5.67 ppm, to be compared with 5.75 and 5.59 ppm in the Mo_2 and MoCo analogues). The $Mn(CO)_4$ oscillator of the molecule gives rise to four strong to medium-intensity C–O stretching bands in the IR spectrum, consistent with the local C_{2v} symmetry of a trigonal pyramidal $[ML(CO)_4]$ complex having a ligand L at an equatorial position.[17]

Table 2. Selected IR,[a] and $^{31}P\{^{1}H\}$ Data[b] for New Compounds.

Compound	ν(CO)	δ_P
$[Mo_2Cp_2(\mu\text{-}\kappa^2\text{:}\kappa^1,\eta^6\text{-SPMes*})(CO)_2]$ (**1**)[c]	1933 (vs), 1848 (s)	124.8
$[MnMoCp(\mu\text{-}\kappa^1\text{:}\kappa^1,\eta^6\text{-PMes*})(CO)_4]$ (**2**)	2018 (vs), 1945 (m, sh), 1930 (s), 1908 (m)	522.5
$[MnMoCp(\mu\text{-}\kappa^2\text{:}\kappa^1,\eta^4\text{-SPMes*})(CO)_5]$ (**3**)	2062 (s), 1975 (vs, br), 1938 (m)	107.6
$[Mn_2Mo_2Cp_2(\mu\text{-}\kappa^1\text{:}\kappa^1,\eta^6\text{-PMes*})(\mu_3\text{-S})(CO)_8]$ (**4**)	2012 (s), 1976 (s), 1946 (vs), 1920 (m, sh), 1897 (w), 1872 (w), 1828 (vw, br)	559.9
$[Mn_2MoCp\{\mu\text{-}\kappa^1\text{:}\kappa^1\text{:}\kappa^1,\eta^5\text{-P}(C_6H_3{}^tBu_3)\}(CO)_8]$ (**5**)	2052 (vs), 1998 (s), 1963 (s), 1945 (w), 1918 (w)	471.3
$[MnMoCp(\mu\text{-}\kappa^2\text{:}\kappa^1,\eta^6\text{-SPMes*})(CO)_4]$ (**6**)	2062 (vs), 1986 (s), 1976 (s), 1936 (m)	126.9

[a] Recorded in dichloromethane solution, with C–O stretching bands [ν(CO)] in cm^{-1}. [b] Recorded in CD_2Cl_2 solution at 162.06 MHz and 295 K unless otherwise stated, with chemical shifts (δ) in ppm relative to external 85% aqueous H_3PO_4. [c] Data taken from reference 11.

M–P Bonding in Compound 2 and Related Phosphinidene-Bridged Complexes. To gain further insight concerning the influence of the heterometal on the degree of delocalization of the π-bonding interaction along the Mo–P–M chain in arylphosphinidene-bridged complexes of type **E** alike to **2**, we have performed DFT calculations on the complexes $[L_nM(\mu\text{-}\kappa^1\text{:}\kappa^1,\eta^6\text{-PMes*})MoCp]$ (ML_n = $MoCp(CO)_2$, $Mn(CO)_4$, $Co(CO)_3$) (see the Experimental Section and Supporting Information -SI- for details),[18] and examined the resulting geometries and frontier molecular orbitals, as well as the electron density at the relevant bonds, as managed by the Atoms in Molecules (AIM) theory.[19] The computed geometrical parameters (Figure 2 and Table 3) are in good agreement with the ones determined by X-ray crystallography, although M–P distances involving the molybdenum atoms are slightly overestimated (by ca. 0.05 Å), a common circumstance in this sort of calculations. Besides this, we should recall that the optimized gas-phase structures are free from any external influence (something not granted in the case of X-ray derived data) and have thus an additional value for comparative purposes. As concerning the Mo–P–M interaction, the optimized geometries follow the trend observed in the X-ray structures, with Mo–PM lengths in the order Co < Mo ≤ Mn, with the difference between the Mn and Co complexes (0.043 Å) being identical to the experimental difference in these lengths (0.044(1) Å). This structural difference points to a genuine change in the π-bonding interaction at these otherwise quite similar molecules.

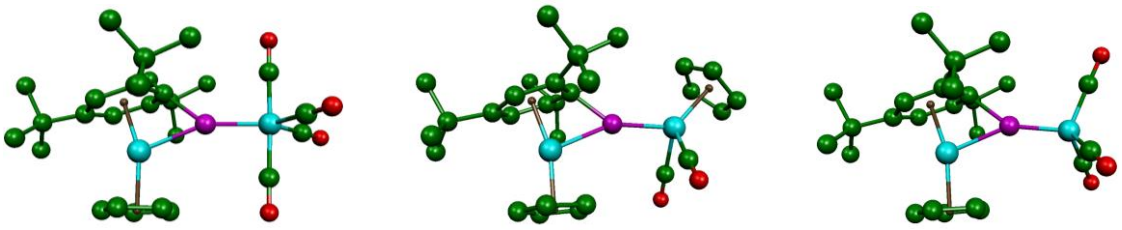

Figure 2. DFT-B3LYP computed structures for compound **2** (left) and its Mo_2 (center) and MoCo (right) analogues, with H atoms omitted.

Table 3. Selected Data for the B3LYP-optimized Geometries of Complexes $[L_nM(\mu\text{-}\kappa^1\text{:}\kappa^1,\eta^6\text{-PMes*})MoCp]^a$

Parameter [b]	MoMn (**2**)	MoMo	MoCo	Exp (**2**)
M–P	2.146	2.271	2.057	2.1414(8)
Mo–P	2.425	2.412	2.382	2.3704(9)
P–C	1.832	1.845	1.835	1.832(3)
Mo–C	2.201	2.216	2.206	2.190(3)
Mo–P–M	156.9	154.1	151.3	158.99(4)
M–P–C	142.7	144.9	147.3	139.77(9)
Mo–P–C	60.4	61.0	61.5	61.23(8)

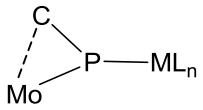

[a] ML_n = $Mn(CO)_4$, $MoCp(CO)_2$, $Co(CO)_3$). [b] Bond lengths (Å) and angles (deg) according to the labeling shown above; see the experimental section for details of DFT calculations.

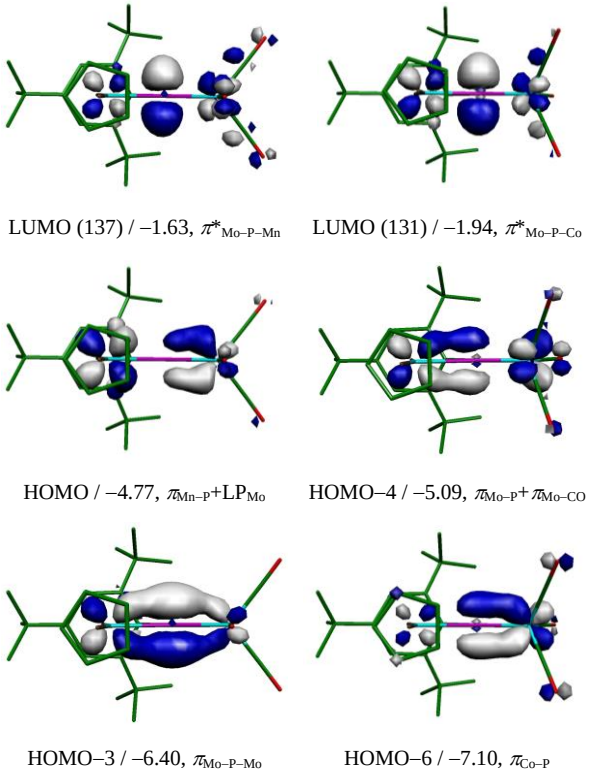

Figure 3. Selected B3LYP-computed molecular orbitals of compound **2** (left) and its MoCo analogue (right), viewed from the Mo–P–M plane, with their energies (in eV) and main bonding character indicated below. See the SI for further information and orbitals of the MoMo analogue.

Inspection of the molecular orbitals describing the π-bonding Mo–P–M interaction in these complexes parallels the geometrical findings, and points to a fully delocalized interaction for the cobalt complex, represented by orbitals HOMO–4 (Mo–P bonding) and HOMO–6 (Co–P bonding), with similar participation of the metal atoms (Figure 3). In the manganese compound **2** this interaction is represented by the HOMO (Mn–P bonding) and HOMO–3 orbital (Mo–P–Mn bonding), this yielding an overall π-interaction more localized on the Mn–P bond, and a similar picture emerges for the

MoMo compound (see the SI), in agreement with their similar geometrical parameters. A more quantitative measurement of these differences, however, is given by the electron density at the Mo–P bond critical point of the Mo–P–M chain in these compounds, with values of 0.552, 0.573 and 0.612 eÅ^{-3} for the MoMn, Mo_2 and MoCo complexes, respectively. As reference figures at this level of calculation we can quote the values of 0.441 and 0.654 eÅ^{-3} computed respectively for the almost single and double Mo–P bonds in the type **E** phosphinidene complex [$Mo_2Cp_2(\mu$-PH)$(CO)_2(\eta^6$-Mes*H)].[13b] It remains to be seen whether the above electronic differences are of consequence to the chemical behavior of these heterometallic species, a matter to be addressed in future investigations.

Structural Characterization of the Thiophosphinidene Complexes 3 and 6. The structure of **3** in the crystal (Figure 4 and Table 4) can be derived from that of **2** after addition of a carbonyl ligand at the Mo atom, and of a sulfur atom on the P–Mn multiple bond, both from the same side of the MoPMn plane. As anticipated, the incorporation of the extra carbonyl causes a slippage of the aryl ring from η^6 to the η^4 coordination mode,[12] reflected in ring folding and detachment of the closer C atoms (C14 and C15; Mo···C > 3.3 Å), which then display a conventional C–C double bond (1.334(6) Å). The addition of the sulfur atom formally reduces the Mn–P bond order from 2 to 1, and accordingly causes a significant increase of ca. 0.15 Å in the Mn–P length, to reach a figure of 2.294(1) Å close to the values of around 2.30 Å commonly found for manganese(I) carbonyl complexes bearing phosphine ligands, but the Mo–P bond seems to be little perturbed along the process (only 0.03 Å higher than that in **2**). Besides this, the P–S length (2.036(1) Å) is somewhat shorter than the reference single-bond value of ca. 2.12 A,[20] and suggestive of the presence of some multiplicity in this bond, while the P atom displays only a modest pyramidalization (Σ_{XPY} ca. 354°). All these structural features have been previously found in related Mo_2 complexes bearing SPR bridging ligands and analyzed with the help of DFT calculations, these revealing the involvement of the S atom in π bonding not only with P but even with the Mo atom of the PSMo cycle.[11] In the case of **3**, the Mn–S distance of 2.430(1) Å almost matches the reference value of 2.44 Å for a single-bond length between these atoms,[20] and therefore suggests the absence of significant π-bonding contribution to the S–Mn interaction. We finally note that this distance is only marginally longer than the values of ca. 2.40 Å previously measured for the dimanganese complexes [$Mn_2(\mu$-κ^1:κ^2-SPR)$(CO)_9$] (R = Me, TMP),[21] which are the only other thiophosphinidene-bridged complexes previously characterized having Mn atoms.

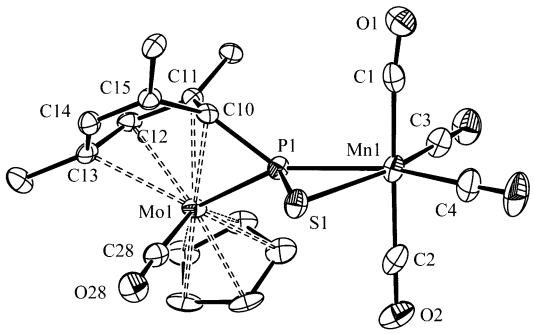

Figure 4. ORTEP diagram (30% probability) of compound **3**, with H atoms and ^{t}Bu groups (except their C^{1} atoms) omitted for clarity.

Table 4. Selected Bond Lengths (Å) and Angles (º) for Compound **3**

Mo1–P1	2.404(1)	Mo1–P1–Mn1	146.29(5)
Mn1–P1	2.294(1)	Mo1–P1–C10	64.6(1)
Mo1–C10	2.296(3)	Mn1–P1–C10	143.0(1)
Mo1–C11	2.238(4)	Mn1–P1–S1	67.99(4)
Mo1–C12	2.267(4)	P1–Mo1–C28	83.8(1)
Mo1–C13	2.469(4)	P1–Mn1–S1	50.97(4)
Mo1–C28	1.972(5)	P1–Mn1–C1	93.5(1)
Mn1–S1	2.430(1)	P1–Mn1–C2	88.6(2)
P1–S1	2.036(1)	P1–Mn1–C3	110.5(2)
P1–C10	1.775(4)	P1–Mn1–C4	150.0(2)
C14–C15	1.334(6)	C3–Mn1–C4	99.5(2)
		C1–Mn1–C2	175.3(2)

Spectroscopic data in solution for **3** are fully consistent with the structure found in the crystal. The phosphorus ligand expectedly gives rise to a considerably shielded ^{31}P NMR resonance (δ_P 107.6 ppm) with a shift comparable to the one measured for the precursor **1** (124.8 ppm), and the C–O stretches of the $Mn(CO)_4$ fragment (2062 (s), 1975 (vs, br), 1938 (m) cm^{-1}) are some 40 cm^{-1} higher than the corresponding stretches in the phosphinidene complex **2**, due to the electron-withdrawing influence of the S atom now bound to manganese. The presence of these strong bands in the IR spectrum precludes the identification of the C–O stretch corresponding to the Mo-bound carbonyl, which is expected around 1960 cm^{-1}.[11] Yet the presence of this ligand is responsible for the η^4-coordination of the aryl ring of the thiophosphinidene ligand, and the latter is clearly established by the appearance, in the ^{1}H NMR spectrum of **3**, of inequivalent CH resonances at 5.71 and 6.07 ppm, with shifts characteristic of coordinated (cf. 5.67 ppm in **2**) and non-coordinated CH groups respectively, as observed previously in related Mo_2 complexes bearing η^4-bound PMes* rings.[11,12]

Complex **6** displays a ^{31}P chemical shift comparable to those of **1** and **3**, and the $Mn(CO)_4$ fragment gives rise to four well-defined C–O stretches in the IR spectrum with frequencies comparable to those of **3**, all of it being indicative of the presence of a *P*:*P*,*S*-bound thiophosphinidene ligand connecting the Mo and Mn atoms. The η^6-coordination of the Mes* ring of the phosphorus ligand is revealed by the low ^{1}H

chemical shift of the ring CH groups (δ_H 5.75 and 5.67 ppm) which, however, are now inequivalent due to the presence of the sulfur atom bound to phosphorus.

Structure of the Sulfide-Bridged Cluster 4. The molecular structure of **4** in the crystal (Figure 5 and Table 5) displays a Mn_2Mo triangle built up from $MoCp(CO)_2$ and $Mn(CO)_3$ fragments, and triply-bridged by a sulfur atom. One of the carbonyls bound to the Mn(2) atom is actually involved in a semibridging interaction with the Mn(1) atom (Mn–C(3) ca. 1.92, 2.25 Å), and the coordination sphere of the Mn(2) atom is completed with the terminal *P*-coordination of a MoCp(κ^1,η^6-PMes*) fragment, much in the same way as found in **2**, thus defining a planar trigonal environment around the P atom. The interatomic distances at the Mo–P–Mn chain (2.354(2) and 2.140(2) Å) are very similar to those measured in **2** (2.3704(9) and 2.1414(8) Å) and therefore indicative of substantial delocalization of the π-bonding interaction of the phosphinidene ligand over this chain, as discussed above.

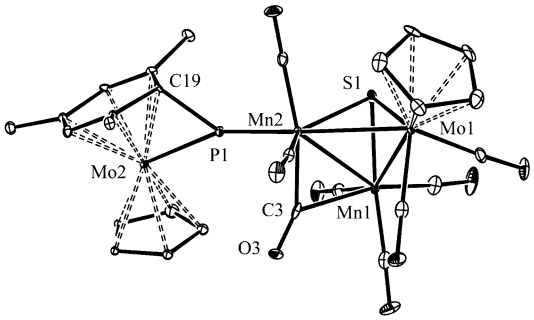

Figure 5. ORTEP diagram (30% probability) of compound **4**, with H atoms and ^{t}Bu groups (except their C^1 atoms) omitted for clarity.

Table 5. Selected Bond Lengths (Å) and Angles (°) for Compound **4**

Mo1–Mn1	2.903(2)	Mo2–P1–Mn2	160.1(1)
Mo1–Mn2	2.849(2)	Mo2–P1–C19	61.7(3)
Mn1–Mn2	2.683(2)	Mn2–P1–C19	136.7(3)
Mo1–S1	2.401(2)	P1–Mn2–Mo1	174.4(1)
Mn1–S1	2.220(3)	P1–Mn2–C3	85.0(3)
Mn2–S1	2.250(2)	P1–Mn2–C7	109.8(3)
Mo2–P1	2.354(2)	P1–Mn2–C8	87.0(3)
Mn2–P1	2.140(2)	C5–Mn1–C3	87.9(4)
Mo2–C19	2.191(8)	C5–Mn1–C4	87.1(4)
Mn1–C3	2.247(10)	C5–Mn1–C6	96.5(5)
Mn2–C3	1.915(11)		
P1–C19	1.824(9)		

As for the central Mn_2Mo cluster in **4** we note that, in a formal sense, it should be considered as an electron precise 48-electron trinuclear cluster (with the phosphinidene fragment and S atoms taken here as 3- and 4-electron donors to the cluster, respectively), which is in agreement with the intermetallic distances of ca. 2.85-2.90 (Mo–Mn) and 2.68 Å (Mn–Mn). Although no related $Mn_xMo_y(\mu_3$-S) cluster appears to have been structurally characterized previously, the above lengths compare reasonably well with the intermetallic separations measured in related *homometallic* clusters, such

as the cation $[Mo_3Cp_3(\mu_3\text{-}S)(CO)_6]^+$ (Mo–Mo ca. 2.09 Å, Mo–S ca. 2.36 Å),[22] and the anion $[Mn_3(\mu_3\text{-}S)_2(CO)_9]^-$ (Mn–Mn ca. 2.77 Å; Mn–S ca. 2.25 Å).[23] The M–S lengths in **2** are comparable to the values found in the mentioned homometallic clusters, and the difference between the Mo–S and Mn–S lengths almost matches the 0.15 Å difference in the covalent radii of Mo and Mn,[20] so it can be concluded that the sulfide ligand in **2** bridges the heterometallic cluster in a symmetrical way.

Spectroscopic data in solution for compound **4** are consistent with the structure in the crystal. The phosphinidene ligand displays a strongly deshielded ^{31}P NMR resonance at 559.9 ppm, some 40 ppm above that of **2**, which is consistent with its trigonal planar environment, and the IR spectrum displays seven C–O stretches, one of them at quite low frequency (1828 cm^{-1}), indicative of retention of a semibridging carbonyl in solution. Finally, the η^6-coordination to Mo of the aryl ring of the phosphorus ligand is denoted by the presence of two inequivalent and shielded resonances (δ_H 5.78, 5.69 ppm) for the aryl CH groups in the ^{1}H NMR spectrum of the complex (cf. 5.67 ppm in **2**).

Structure and Bonding in the Phosphinidene-Bridged Cluster 5. The molecule of **5** in the crystal (Figure 6 and Table 6) displays a V-shaped $MoMn_2$ skeleton built up from MoCp and $Mn(CO)_4$ fragments and bridged by the P atom of a phosphinidene ligand, while the former aryl ring of the latter bears now an H atom *endo* positioned at one of the *ortho* carbons (C15), no longer coordinated (Mo–C > 2.90 Å), whereby the ring has been effectively transformed into a sort of η^5-bound cyclohexadienyl ligand bound to Mo (Mo–C 2.20-2.45 Å). The heavy atoms define a moderately puckered central $MoMn_2P$ rhombus (Mo–Mn–P–Mn ca. 159º).

Cluster **5** has 50 valence electrons, and therefore two metal-metal single bonds are to be expected for this molecule, which is fully consistent with the intermetallic Mn–Mn separation of 2.9223(5) Å, very close to that measured in the archetypal $[Mn_2(CO)_{10}]$ (2.9031(2) Å).[24] The Mn2–Mo1 distance of 3.2910(5) Å, however, is significantly longer than expected for a single bond between these atoms (cf. 2.9909(4) Å in the type **D** complex $[MoMnCp\{\mu\text{-}P(TMP)\}(CO)_6]$[4] or ca. 3.08 Å in $[MoMnCp(CO)_8]$.[25] This might be due to steric repulsions between the metallocene and Mn2 fragments, also suggested from the significant deviation of the axial carbonyls bound to Mn2, away from the metallocene fragment (C6–Mn2–C5 ca. 165º). In any case, the weak Mo–Mn2 binding seems to be balanced (as concerning the Mo atom) by a stronger binding of the phosphinidene ligand to Mo, which unexpectedly displays a quite short Mo–P distance of 2.3152(6) Å, actually ca. 0.05 Å shorter than the corresponding separation in **2**, and therefore indicative of the presence of multiple bonding, which seems to be extended to the P–Mn1 connection, as the latter also displays a relatively short separation of 2.1999(7) Å. These distances are actually quite close to the corresponding figures of

2.2912(5) and 2.1862(6) Å measured in the type **D** complex [MoMnCp{μ-P(TMP)}$(CO)_6$],[4] a molecule for which M–P bond orders close to 1.5 should be proposed. In line with this, the P atom shows no significant pyramidalization, since Mo1, Mn1, P and C14 atoms remain almost in the same plane (Σ_{XPY} = 360º). While the latter is itself a common structural feature of μ_3-PR ligands bridging open V-shaped trimetal cores,[26] it certainly allows for the occurrence of delocalized π-bonding interactions. However, in contrast with the strong bonding along the Mo–P–Mn1 chain, the binding of the phosphinidene atom to the Mn2 atom seems substantially weaker, as judged from the ca. 0.15 Å longer P–Mn2 separation (2.3152(6) Å). We might conceal all this structural information by viewing cluster **5** as derived from the interaction of an anionic allyl-like fragment $L_nMo–PR–Mn(CO)_4$ (having a π-bonding interaction delocalized along the Mo–P–Mn1 chain) with a $Mn(CO)_4^+$ cation. To support this interpretation, we have examined the structure and molecular orbitals of **5** using DFT methods.

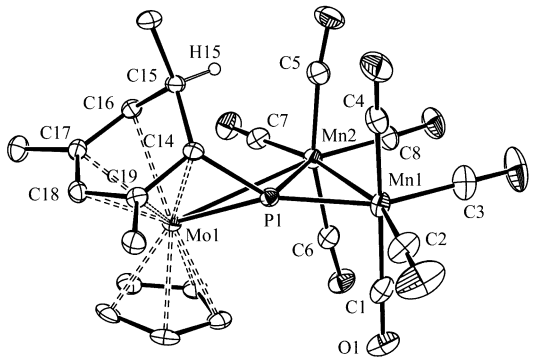

Figure 6. ORTEP diagram (30% probability) of compound **5**, with H atoms and ^{t}Bu groups (except their C^1 atoms) omitted for clarity.

Table 6. Selected Bond Lengths (Å) and Angles (º) for Compound **5**.

Mo1–Mn2	3.2910(5)	Mo1–Mn2–Mn1	90.45(1)
Mn1–Mn2	2.9223(5)	Mo1–P1–Mn1	156.21(3)
Mo1–P1	2.3152(6)	Mo1–P1–C14	63.34(7)
Mn1–P1	2.1999(7)	Mn1–P1–C14	140.45(8)
Mn2–P1	2.3475(6)	Mo1–P1–Mn2	89.79(2)
Mo1–C14	2.205(2)	Mn1–P1–Mn2	79.90(2)
Mo1–C16	2.446(2)	P1–Mn1–C1	90.98(9)
Mo1–C17	2.394(2)	P1–Mn1–C2	113.5(1)
Mo1–C18	2.298(2)	P1–Mn1–C3	145.1(1)
Mo1–C19	2.227(2)	C1–Mn1–C4	174.2(1)
P1–C14	1.801(2)	P1–Mn2–C6	97.53(8)
		P1–Mn2–C7	118.99(9)
		P1–Mn2–C8	139.66(9)
		C5–Mn2–C6	165.0(1)

The overall structural parameters computed for **5** (Figure 7) are in good agreement with the X-ray structure, including the carbonyl distortion around Mn2 discussed above (C6–Mn2–C5 ca. 167º), although the interatomic lengths involving metal atoms are overestimated as usual, particularly as concerning the large Mo–Mn2 separation of

3.4247 Å (exp. 3.2910(5) Å). Yet the computed molecular orbitals give support to our view of **5** as derived from the interaction of an allyl-like fragment $L_nMo–PR–Mn(CO)_4$ to a $Mn(CO)_4^+$ cation, nicely represented by the HOMO (π-type interaction with the acceptor fragment leading to Mn1–Mn2 and weaker Mo1–Mn2 bonding) and HOMO–10 orbitals (σ-type interaction with the acceptor, mainly accounting for the P–Mn2 bond and residual Mo–P–Mn1 π-bonding) (Figure 7). A more quantitative evidence for the retention of significant π-bonding along the Mo–P–Mn1 chain in **5** is given by the electron densities at the corresponding bond critical points, with values of 0.609 and 0.530 eÅ^{-3} respectively, which are comparable to those computed for **2** (0.552 and 0.629 eÅ^{-3} respectively). Moreover these figures actually reveal a drift of electron density from the Mn1–P bond to the P–Mo bond, surely to balance the weak Mo–Mn2 bonding, as noted above.

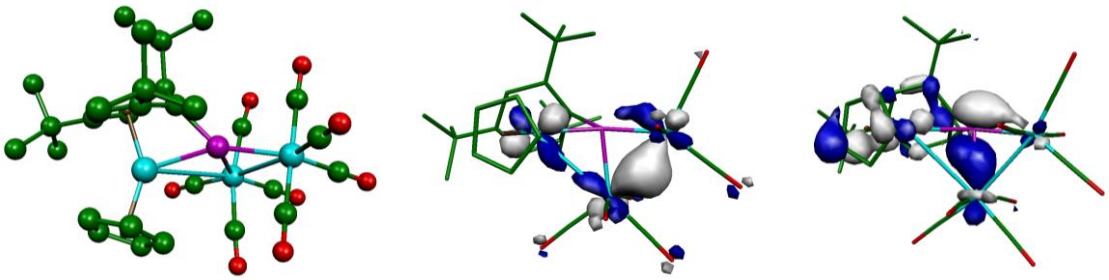

Figure 7. DFT-B3LYP computed structure for compound **7**, with H atoms omitted (left). Selected bond lengths (A): Mo1–Mn2 = 3.4247, Mn1–Mn2 = 2.9915, Mo1–P1 = 2.3603, Mn1–P1 = 2.2466, Mn2–P1= 2.3911, with labeling as in Figure 6. The orbitals mainly describing the interaction between the allyl-like Mo–P–Mn1 fragment and the $Mn(CO)_4$ cation are shown at the middle (HOMO, –5.40 eV) and on the right (HOMO–10, –7.50 eV).

Spectroscopic data in solution for compound **5** are fully consistent with the structure found in the crystal and deserve only a few comments. Its IR spectrum shows seven C–O stretches when recorded in petroleum ether, which is consistent with the presence of a $Mn_2(CO)_8$ oscillator and the absence of symmetry elements. Surprisingly, the ^{31}P NMR spectrum displays a relatively deshielded phosphinidene resonance at 471 ppm, only 40 ppm more shielded than the corresponding resonance in **2**, in spite of the change operated in the coordination mode of the phosphorus ligand (from μ_2 to μ_3). This is obviously related to the retention of substantial π-bonding interaction along the Mo–P–Mn1 chain, as discussed above, which is a critical element behind the strong deshielding characteristic of binuclear complexes bearing trigonal phosphinidene ligands.[3] Finally, the η^5-coordination of the C_6 ring of the phosphinidene ligand is denoted by the appearance in the ^1H NMR spectrum of inequivalent and relatively shielded CH resonances at 5.65 and 5.04 ppm (cf. 5.67 ppm in **2**), while the *endo* proton incorporated at the *ortho* carbon of the ring gives rise to a quite shielded resonance at 2.08 ppm, as expected for an aliphatic H atom.

Concluding Remarks

The photochemical reactions of the thiophosphinidene Mo_2 complex **1** with $[Mn_2(CO)_{10}]$ provide a reasonable synthetic access to novel heterometallic phosphinidene derivatives featuring Mo–P=Mn connections of type **E** which, however, display substantial delocalization of the π-bonding interaction over both metal atoms. The available structural data, as well as DFT calculations carried out on some of these heterometallic products and related species, indicate that the extent of such a delocalization is significantly dependent on the heterometal fragment involved, with $Co(CO)_3$ yielding the largest delocalization and $Mn(CO)_4$ the smallest, yet a significant one. The dominant reaction pathway in the photochemical reactions of **1** with $[Mn_2(CO)_{10}]$ involves the eventual replacement of the $SMoCp(CO)_2$ fragment in the parent compound with a $Mn(CO)_4$ fragment, but incorporation of an additional manganese fragment takes place when performing the photolysis in tetrahydrofuran solution, this triggering an H-atom abstraction at the aryl ring of the phosphinidene ligand which renders a rare 9-electron donor cyclohexadienylidene-phosphinidene ligand. The subtleness of all these photochemical reactions is further indicated by the fact that the photochemical reaction of the thiophosphinidene complex $[Mo_2Cp_2(\mu\text{-}\kappa^2\text{:}\kappa^1,\eta^4\text{-SPMes*})(CO)_3]$ with $[Mn_2(CO)_{10}]$ also results in selective Mo/Mn transmetallation, but now with retention of the sulfur atom to yield the corresponding thiophosphinidene-bridged MoMn derivative.

Experimental Section

General Procedures and Starting Materials. All manipulations and reactions were carried out under an argon (99.995%) atmosphere using standard Schlenk techniques. Some experiments were carried out using Schlenk tubes equipped with Young´s valves. Solvents were purified according to literature procedures and distilled prior to use.[27] Petroleum ether refers to that fraction distilling in the range 338-343 K. Compounds $[Mo_2Cp_2(\mu\text{-}\kappa^1\text{:}\kappa^1,\eta^6\text{-PMes*})(CO)_2]$,[12b] $[Mo_2Cp_2(\mu\text{-}\kappa^2\text{:}\kappa^1,\eta^6\text{-SPMes*})(CO)_2]$ (**1**),[11] and $[Mo_2Cp_2(\mu\text{-}\kappa^2\text{:}\kappa^1,\eta^4\text{-SPMes*})(CO)_3]$[11] were prepared as described previously (Mes* = 2,4,6-$C_6H_2{}^tBu_3$), while all other reagents were obtained from the usual commercial suppliers and used as received, unless otherwise stated. Photochemical experiments were performed using jacketed quartz or Pyrex Schlenk tubes cooled by tap water (ca. 288 K). A 400 W medium-pressure mercury lamp placed ca. 1 cm away from the Schlenk tube was used for these experiments. Chromatographic separations were carried out using jacketed columns cooled by tap water. Commercial aluminum oxide (activity I, 70-290 mesh) was degassed under vacuum prior to use. The latter was mixed under argon with the appropriate amount of water to reach activity IV. IR C–O stretching

frequencies were measured in solution, are referred to as ν(CO) (solvent), and are given in cm^{-1}. Nuclear magnetic resonance (NMR) spectra were routinely recorded at 400.13 MHz (^{1}H) or 162.06 MHz (^{31}P) in CD_2Cl_2 solutions at 295 K, unless otherwise stated. Chemical shifts (δ) are given in ppm, relative to internal tetramethylsilane (^{1}H), or external 85% aqueous H_3PO_4 (^{31}P), and coupling constants (J) are given in Hz.

Photochemical Reaction of 1 with [$Mn_2(CO)_{10}$] in Toluene Solution. A toluene solution (12 mL) of compound **1** (0.050 g, 0.073 mmol) and [$Mn_2(CO)_{10}$] (0.080 g, 0.205 mmol) was irradiated with visible-UV light at 288 K for 3 h in a quartz Schlenk tube while gently bubbling argon through the solution, to give a brown-orange solution. The solvent was then removed under vacuum, the residue was extracted with a minimum of dichloromethane/petroleum ether (1/2) and the extract was chromatographed through alumina. Elution with dichloromethane/petroleum ether (1/6) gave a red-orange fraction yielding, after removal of solvents, compound [MnMoCp(μ-κ^1:κ^1,η^6-PMes*)$(CO)_4$] (**2**) as an orange solid (0.026 g, 60%). Elution with dichloromethane/petroleum ether (1/5) gave a yellow-orange fraction yielding analogously compound **3** (see below) as a yellow solid (0.005 g, 10%). Finally, elution with dichloromethane/petroleum ether (2/1) gave a turquoise fraction yielding analogously compound [$Mn_2Mo_2Cp_2$(μ-κ^1:κ^1,η^6-PMes*)(μ_3-S)$(CO)_8$] (**4**) as a blue solid (0.014 g, 20%). The crystals of **2** and **3** used in the X-ray diffraction studies were grown by the slow diffusion at 253 K of layers of diethyl ether and petroleum ether into dichloromethane solutions of the corresponding complexes. Crystals of **4** were grown analogously, but using toluene instead of diethyl ether. *Data for compound **2***: Anal. Calcd for $C_{27}H_{34}MnMoO_4P$: C, 53.65; H, 5.67. Found: C, 53.52; H, 5.62. ν(CO) (petroleum ether): 2029 (vs), 1960 (m), 1940 (vs), 1932 (s). ^{1}H NMR: δ 5.67 (s, 2H, C_6H_2), 5.30 (d, J_{HP} = 2, 5H, Cp), 1.32 (s, 18H, ^{t}Bu), 1.20 (s, 9H, ^{t}Bu). *Data for compound **4***: Anal. Calcd for $C_{36}H_{39}Mn_2Mo_2O_8PS$: C, 44.83; H, 4.08; S, 3.32. Found: C, 44.62; H, 4.03; S, 3.25. ν(CO) (petroleum ether): 2022 (vs), 1974 (s), 1960 (s), 1952 (m, sh), 1925 (w), 1907 (w), 1831 (vw, br). ^{1}H NMR: δ 5.78, 5.69 (2d, J_{HP} = 1, 2 x 1H, C_6H_2), 5.47 (s, br, 5H, Cp), 5.24 (s, 5H, Cp), 1.42, 1.23, 1.16 (3s, 3 x 9H, ^{t}Bu).

Preparation of [MnMoCp(μ-κ^2:κ^1,η^4-SPMes*)$(CO)_5$] (3). A toluene solution (10 mL) of compound [Mo_2Cp_2(μ-κ^2:κ^1,η^4-SPMes*)$(CO)_3$] (0.030 g, 0.042 mmol) and [$Mn_2(CO)_{10}$] (0.090 g, 0.231 mmol) was irradiated with visible-UV light at 288 K for 2 h in a Pyrex Schlenk tube to give an orange solution. Solvent was then removed under vacuum, the residue was extracted with a minimum of dichloromethane/petroleum ether (1/2) and the extract was chromatographed through alumina. Elution with dichloromethane/petroleum ether (1/5) gave a yellow-orange fraction yielding, after removal of solvents, compound **3** as a yellow solid (0.024 g, 85%). Anal. Calcd for $C_{28}H_{34}MnMoO_5PS$: C, 50.61; H, 5.16; S, 4.83. Found: C, 50.45; H, 5.13; S, 4.75.

ν(CO) (petroleum ether): 2063 (m), 1992 (m), 1979 (vs), 1943 (m). ^{1}H NMR: δ 6.07 (s, 1H, C_6H_2), 5.71 (d, J_{HP} = 5, 1H, C_6H_2), 5.28 (d, J_{HP} = 2, 5H, Cp), 1.47, 1.062, 1.059 (3s, 3 x 9H, ^{t}Bu).

Preparation of [$Mn_2MoCp\{\mu$-κ^1:κ^1,η^5-$P(C_6H_3{}^tBu_3)\}(CO)_8$] (5). A tetrahydrofuran solution (15 mL) of compound **1** (0.030 g, 0.044 mmol) and [$Mn_2(CO)_{10}$] (0.080 g, 0.206 mmol) was irradiated with visible-UV light at 288 K for 3 h in a Pyrex Schlenk tube while gently bubbling argon through the solution, to give a brown solution. Solvent was then removed under vacuum, the residue was extracted with a minimum of dichloromethane/petroleum ether (1/2) and the extract was chromatographed through alumina. Elution with dichloromethane/petroleum ether (1/7) gave an orange fraction yielding, after removal of solvents, compound **5** as an orange solid (0.024 g, 71%). The crystals used in the X-ray diffraction study were grown by the slow diffusion at 253 K of layers of diethyl ether and petroleum ether into a dichloromethane solution of the compound. Anal. Calcd for $C_{31}H_{35}Mn_2MoO_8P$: C, 48.21; H, 4.57. Found: C, 48.50; H, 4.60. ν(CO) (petroleum ether): 2055 (s), 2002 (s), 1985 (w), 1968 (vs), 1954 (w), 1947 (vw), 1927 (w). ^{1}H NMR: δ 5.65 (s, br, 1H, C_6H_3), 5.24 (s, 5H, Cp), 5.04 (dd, J_{HH} = 6, 2, 1H, C_6H_3), 2.08 (dd, J_{HP} = 11, J_{HH} = 6, 1H, C_6H_3), 1.38, 1.29, 0.70 (3s, 3 x 9H, ^{t}Bu).

Preparation of [$MnMoCp(\mu$-κ^2:κ^1,η^6-PMes*)$(CO)_4$] (6). A dichloromethane solution of S_8 (1.0 mL of a 0.188 M solution, 0.188 mmol) was added to a dichloromethane solution (3 mL) of compound **2** (0.020 g, 0.033 mmol) and the mixture was stirred at room temperature for 30 min to give an orange solution. Solvent was then removed under vacuum, the residue was extracted with a minimum of dichloromethane/petroleum ether (1/4) and the extract was chromatographed through alumina. Elution with dichloromethane/petroleum ether (1/9) gave an orange fraction yielding, after removal of solvents, compound **6** as an orange solid (0.018 g, 86%). Anal. Calcd for $C_{27}H_{34}MnMoO_4PS$: C, 50.95; H, 5.38; S, 5.04. Found: C, 50.67; H, 5.25; S, 4.90. ν(CO) (petroleum ether): 2065 (s), 1995 (s), 1977 (vs), 1946 (vs). ^{1}H NMR: δ 5.75 (dd, J_{HP} = 3, J_{HH} = 1, 1H, C_6H_2), 5.67 (d, J_{HH} = 1, 1H, C_6H_2), 5.10 (d, J_{HP} = 3, 5H, Cp), 1.47, 1.43, 1.24 (3s, 3 x 9H, ^{t}Bu).

X-ray Structure Determination of Compounds 2-5. Data collection was performed at 150 K (**2**, **3**, **5**) or 100 K (**4**) on an Oxford Diffraction Xcalibur Nova single crystal diffractometer, using Cu-Kα radiation. Images were collected at a 63 mm fixed crystal-detector distance, using the oscillation method, with 1º oscillation and variable exposure time per image. Data collection strategy was calculated with the program *CrysAlis Pro CCD*,[28] and data reduction and cell refinements were performed with the program *CrysAlis Pro RED*.[28] An empirical absorption correction was applied using the SCALE3 ABSPACK algorithm as implemented in the latter program. Using the program suite

WINGX,[29] the structures were solved by Patterson interpretation and phase expansion using SHELXL2016, and refined with full-matrix least squares on F^2 using SHELXL2016,[30] to give the residuals collected in Table 7. In general, all non-hydrogen atoms were refined anisotropically and all hydrogen atoms were geometrically placed and refined using a riding model. However, C atoms involved in disorder (see below) were refined isotropically to prevent their temperature factors from becoming non-positive definite. Complex **2** crystallized with half a molecule of *n*-hexane placed on a symmetry element; moreover, one ^{t}Bu group and one Cp ligand were disordered over two sites, satisfactorily refined with 0.5/0.5 and 0.6/0.4 occupancies, respectively. For complex **5**, the atoms H15, H16 and H18 were located on difference maps and refined isotropically. Complex **4** crystallized with a molecule of toluene; moreover one Cp ligand and one ^{t}Bu group were disordered over two sites, satisfactorily refined with 0.5/0.5 occupancies; yet, due to the poor quality of the diffraction data (likely unsolved twinning), large electron density residuals (maximum ca. 9 eÅ^{-3}) remained in the vicinity of the metal atoms.

Table 7. Crystal Data for New Compounds

	2·1/2C_6H_{14}	**3**	**4**·C_7H_8	**5**
mol formula	$C_{30}H_{41}MnMoO_4P$	$C_{28}H_{34}MnMoO_5PS$	$C_{43}H_{47}Mn_2Mo_2O_8PS$	$C_{31}H_{35}Mn_2MoO_8P$
mol wt	647.48	664.47	1056.61	772.38
cryst syst	monoclinic	monoclinic	monoclinic	monoclinic
space group	*P* $2_1/n$	*P* $2_1/n$	*P* $2_1/c$	*C* 2/*c*
radiation (λ, Å)	1.54184	1.54184	1.54184	1.54184
a, Å	15.1918(2)	10.3604(3)	15.8152(6)	32.1859(3)
b, Å	12.86900(10)	16.9854(5)	9.6336(7)	11.41250(10)
c, Å	16.8870(2)	16.7659(5)	28.7313(15)	18.4516(2)
α, deg	90	90	90	90
β, deg	114.132(2)	96.524(3)	105.760(5)	102.7550(10)
γ, deg	90	90	90	90
V, Å^3	3012.94(7)	2931.28(15)	4212.9(4)	6610.42(11)
Z	4	4	4	8
calcd density, g cm^{-3}	1.427	1.506	1.666	1.552
absorp coeff, mm^{-1}	7.570	8.475	10.784	10.035
temperature, K	150.0(1)	150(2)	99.8(8)	150.0(1)
θ range (deg)	3.303-74.881	3.717-74.642	2.903-72.457	2.815-74.759
index ranges (*h*, *k*, *l*)	–18, 18; –15, 15; –21, 20	–12, 12; –20, 20; –20, 14	–19, 18; –8, 11; –32, 35	–39, 40; –14, 13; –21, 22
no. of reflns collected	17195	11155	15002	25334
no. of indep reflns (R_{int})	6007 (0.043)	5729 (0.040)	8050 (0.1497)	6636 (0.034)
reflns with $I > 2\sigma(I)$	5494	4903	6774	6250
R indexes [data with $I > n\sigma(I)$][a]	R_1 = 0.0387 wR_2 = 0.1037[b]	R_1 = 0.0473 wR_2 = 0.1360[c]	R_1 = 0.1171 wR_2 = 0.2548[d]	R_1 = 0.0278 wR_2 = 0.0818[e]
R indexes (all data)[a]	R_1 = 0.0387 wR_2 = 0.1037[b]	R_1 = 0.0554 wR_2 = 0.1437[c]	R_1 = 0.1680 wR_2 = 0.3784[d]	R_1 = 0.0298 wR_2 = 0.0836[e]
GOF	1.072	1.113	1.706	1.091
no. of restraints/parameters	0 / 321	0 / 343	4 / 496	0 / 406
$\Delta\rho$(max., min.), eÅ^{-3}	1.186 / –0.819	0.888 / –1.192	8.828 / –5.727	0.369 / –0.931
CCDC deposition No	1583271	1583272	1583273	1583274

[a] $R = \Sigma||F_o| - |F_c|| / \Sigma|F_o|$; $wR = [\Sigma(|F_o| - |F_c|)^2 / \Sigma|F_o|^2]^{1/2}$; [b] $R = \Sigma||F_o| - |F_c|| / \Sigma|F_o|$; $wR = [\Sigma w(|F_o|^2 - |F_c|^2)^2 / \Sigma w|F_o|^2]^{1/2}$; $w = 1/[\sigma^2(F_o^2) + (aP)^2 + bP]$ where $P = (F_o^2 + 2F_c^2)/3$; [b] a = 0.0631, b = 1.8453. [c] a = 0.0809, b = 1.5051. [d] a = 0.2000P, b = 0.0000. [e] a = 0.0485, b = 6.0132.

Computational Details. All DFT computations were carried out using the GAUSSIAN03 package,[31] in which the hybrid method B3LYP was used with the Becke three-parameter exchange functional[32] and the Lee-Yang-Parr correlation functional.[33] A pruned numerical integration grid (99,590) was used for all the calculations *via* the keyword Int=Ultrafine. Effective core potentials and their associated double-ζ LANL2DZ basis set were used for the metal atoms.[34] The lighter elements (O, C, N and H) were described with the 6-31G* basis,[35] and the P atom with the 6-311+G* basis.[36] Geometry optimizations were performed under no symmetry restrictions, and frequency analyses were performed for all the stationary points to ensure that minimum structures with no imaginary frequencies were achieved. Molecular graphics and vibrational modes were visualized using the Molekel program.[37] The Atoms-in-Molecules analysis was carried out using the MultiWFN program.[38] The structures of compound **2** and its Mo_2 and MoCo analogues were also optimized with the meta-GGA functional M06L of Zhao and Truhlar, specifically designed to take into account noncovalent attractions and

dispersion effects through extensive parametrization using several training sets containing transition metal complexes,[39] and the hybrid meta-GGA functional ωB97XD, which contains empirical dispersion terms and also long-range corrections.[40] As expected, the computed distances involving the metal atoms were now closer to the experimental distances in general (see the SI), but the overall picture remained the same. However, these functionals did not perform better than B3LYP at reproducing the *differences* in the corresponding Mo–P lengths, which is a central point under discussion in our work.

Supporting Information. A CIF file containing full crystallographic data for compounds **2** to **5** (CCDC 1583271-1583274), a PDF file containing results of DFT calculations (structures, molecular orbitals and electron density properties), and an XYZ file including the Cartesian coordinates for all computed species. This material is available free of charge *via* the Internet at http://pubs.acs.org.

Author Information. Corresponding authors: E-mail: garciavdaniel@uniovi.es (D. G. V.), mara@uniovi.es (M. A. R). The authors declare no competing financial interest.

Acknowledgment. We thank the Gobierno del Principado de Asturias for financial support (Project GRUPIN14-011), the MINECO of Spain and FEDER for financial support (Project CTQ2015-63726-P), and the CMC and X-ray Units of the Universidad de Oviedo for access to computing facilities and acquisition of diffraction data, respectively.

References

1. (*a*) Dillon, K. B.; Mathey, F.; Nixon, J. F. *Phosphorus: The Carbon-Copy*; Wiley: Chichester, 1998. (*b*) *Multiple Bonds and Low Coordination in Phosphorus Chemistry*, Regitz, M.; Scherer, O. J. (Eds.), Georg Thieme Verlag: Sttugart, 1990. (c) Balász, G. Gregoriades, L. J.; Scheer, M. Triple Bonds between Transition Metals and the Heavier Elements of Groups 14 and 15. *Organometallics* **2007**, *26*, 3058-3075.
2. Recent reviews: (a) Mathey, F.; Duan, Z. Activation of A–H bonds (A = B, C, N, O, Si) by using monovalent phosphorus complexes [RP→M]. *Dalton Trans.* **2016**, *45*, 1804-1809. (b) Aktas, H.; Slootweg, J. C.; Lammertsma, K. Nucleophilic phosphinidene complexes: access and applicability. *Angew. Chem. Int. Ed.* **2010**, *49*, 2102-2113. (c) Waterman, R. Metal-phosphido and -phosphinidene complexes in P–E bond-forming reactions. *Dalton Trans.* **2009**, 18-26. (d) Mathey, F. Developing the chemistry of monovalent phosphorus. *Dalton Trans.* **2007**, 1861-1868. (e) Lammertsma, K. Phosphinidenes. *Top. Curr. Chem.* **2003**, *229*, 95-119. (f) Lammertsma, K.; Vlaar, M. J. M. Carbene-Like Chemistry of Phosphinidene

Complexes − Reactions, Applications, and Mechanistic Insights. *Eur. J. Org. Chem.* **2002**, 1127-1138. (g) Streubel, R. Chemistry of λ^3-2*H*-azaphosphirene metal complexes. *Coord. Chem. Rev.* **2002**, *227*, 175-192. (h) Mathey, F.; Tran Huy, N. H.; Marinetti, A. Electrophilic Terminal-Phosphinidene Complexes: Versatile Phosphorus Analogues of Singlet Carbenes. *Helv. Chim. Acta* **2001**, *84*, 2938-2957. (i) Stephan, D. W. Zirconium – Phosphorus Chemistry: Strategies in Syntheses, Reactivity, Catalysis, and Utility. *Angew. Chem. Int. Ed.* **2000**, *39*, 314–329. (j) Shah, S.; Protasiewicz, J. D. 'Phospha-variations' on the themes of Staudinger and Wittig: phosphorus analogs of Wittig reagents. *Coord. Chem. Rev.* **2000**, *210*, 181-201.

3. (a) García, M. E.; García-Vivó, D.; Ramos, A.; Ruiz, M. A. Phosphinidene-bridged binuclear complexes. *Coord. Chem. Rev.* **2017**, *330*, 1-36. (b) Huttner, G.; Evertz, K. Phosphinidene complexes and their higher homologues. *Acc. Chem. Res.* **1986**, *19*, 406-413.
4. Sánchez-Nieves, J.; Sterenberg, B. T.; Udachin, K. A.; Carty, A. J. The reactivity of terminal chloraminophosphido ligands towards metal carbonyl complexes. Formation of μ_2- and μ_3-phosphinidene clusters. *Inorg. Chim. Acta* **2003**, *350*, 486-494.
5. Lang, H.; Winter, M.; Leise, M.; Walter, O.; Zsolnai, L. Stepwise formation of chiral clusters via σ^3,λ^4-phosphanediyl compounds of type (R)(η^1-C_5Me_5)P=ML_n. *J. Chem. Soc., Chem. Commun.* **1994**, 595-596.
6. Hirth, U. A.; Malisch, W. Phosphenium-Übergangsmetallkomplexe XX. Stabilisierung von Mesitylphosphiniden durch ein $Cp(CO)_2W$- und ein $Cp(CO)_2Fe$-Fragment. *J. Organomet. Chem.* **1992**, *439*, C16-C19.
7. Alvarez, B.; Alvarez, M. A.; Amor, I.; García, M. E.; Ruiz, M. A. A Thiophosphinidene Complex as a Vehicle in Phosphinidene Transmetallation: Easy Formation and Cleavage of a P–S Bond. *Inorg. Chem.* **2011**, *50*, 10561-10563.
8. Alvarez, B.; Alvarez, M. A.; García, M. E.; Ruiz, M. A. P–S bond cleavage in reactions of thiophosphinidene-bridged dimolybdenum complexes with $[Co_2(CO)_8]$ to give phosphinidene-bridged heterometallic derivatives. *Dalton Trans.* **2016**, *45*, 1937-1952.
9. (a) Zhang, H. T.; Brown, T. L. Photochemical formation and thermal rearrangements of $Mn_2(CO)_9PR_3$ and $Mn_2(CO)_8(PR_3)_2$. *J. Am. Chem. Soc.* **1993**, *115*, 107-117. (b) Geoffroy, G. L.; Wrighton, M. S. *Organometallic Photochemistry*; Academic Press: London, U. K., 1979, chapter 2.
10. (a) *Paramagnetic Organometallic Species in Activation / Selectivity, Catalysis.* Chanon, M.; Julliard, M.; Poite, J. C., Eds.; Kluwer Academic Publishers: Dordrecht, 1989. (b) *Organometallic Radical Processes.* Trogler, W. C., Ed.;

Elsevier: Amsterdam, 1990. (c) Astruc, D. *Electron Transfer and Radical Processes in Transition-Metal Chemistry*; VCH: New York, 1995.

11. Alvarez, B.; Alvarez, M. A.; Amor, I.; García, M. E.; García-Vivó, D.; Ruiz, M. A.; Suárez, J. Dimolybdenum Cyclopentadienyl Complexes with Bridging Chalcogenophosphinidene Ligands. *Inorg. Chem.* **2012**, *51*, 7810-7824.
12. (a) García, M. E.; Riera, V.; Ruiz, M. A.; Sáez, D.; Hamidov, H.; Jeffery, J. C.; Riis-Johannessen, T. Ten-electron coordination and reactivity of an arylphosphinidene ligand. *J. Am. Chem. Soc.* **2003**, *125*, 13044-13045. (b) Amor, I.; García, M. E.; Ruiz, M. A.; Sáez, D.; Hamidov, H.; Jeffery, J. C. Formation and Cleavage of P–C, Mo–C, and C–H Bonds Involving Arylphosphinidene and Cyclopentadienyl Ligands at Dimolybdenum Centers. *Organometallics* **2006**, *25*, 4857-4869.
13. (a) Alvarez, M. A.; Amor, I.; García, M. E.; García-Vivó, D.; Ruiz, M. A. Carbene- and Carbyne-like Behavior of the Mo–P Multiple Bond in a Dimolybdenum Complex Inducing Trigonal Pyramidal Coordination of a Phosphinidene Ligand. *Inorg. Chem.* **2007**, *46*, 6230-6232. (b) Alvarez, M. A.; Amor, I.; García, M. E.; García-Vivó, D.; Ruiz, M. A.; Suárez, J. Structure, Bonding and Reactivity of Binuclear Complexes having Asymmetric Trigonal Phosphinidene Bridges: Addition of 16-electron Metal Carbonyl Fragments to the Dimolybdenum Compounds $[Mo_2Cp(\mu\text{-}\kappa^1\text{:}\kappa^1,\eta^5\text{-}PC_5H_4)(CO)_2L]$ and $[Mo_2Cp_2(\mu\text{-}PH)(CO)_2L]$ (L = η^6-1,3,5-$C_6H_3{}^tBu_3$). *Organometallics* **2010**, *29*, 4384-4395.
14. Alvarez, M. A.; Amor, I.; García, M. E.; García-Vivó, D.; Ruiz, M. A.; Suárez, J. Sn–H Bond Additions to Asymmetric Trigonal Phosphinidene-Bridged Dimolybdenum Complexes. *RSC Adv.* **2017**, *7*, 33293-33304.
15. Lang, H.; Leise, M.; Emmerich, C. $[(2,4,6\text{-}{}^tBu_3C_6H_2O)(C_5Me_5)]P{=}Mn(CO)_4$: Ein stabiler λ^4-phosphandiyl-komplex mit phosphor-mangan-mehrfachbindung. *J. Organomet. Chem.* **1991**, *418*, C9-C13.
16. Graham, T. W.; Udachin, K. A.; Carty, A. J. Reactivity of electrophilic μ-phosphinidene complexes with heterocumulenes: formation of the first σ-π-aminophosphaimine complexes $[Mn_2(CO)_8\{\mu\text{-}\eta^1,\eta^2\text{-}P(N^iPr_2){=}NR\}]$ and diazoalkane insertions into metal-phosphorus bonds. *Chem. Commun.* **2005**, 4441-4443.
17. Braterman, P. S. *Metal Carbonyl Spectra*; Academic Press: London, U. K., 1975.
18. (a) Cramer, C. J. *Essentials of Computational Chemistry, 2nd Ed.*; Wiley: Chichester, UK, 2004. (b) Koch, W.; Holthausen, M. C. *A Chemist´s Guide to Density Functional Theory, 2nd Ed.*; Wiley-VCH: Weinheim, 2002.
19. Bader, R. F. W. *Atoms in molecules-A Quantum Theory*; Oxford University Press: Oxford, U. K., 1990.

20. Cordero, B.; Gómez, V.; Platero-Prats, A. E.; Revés, M.; Echevarría, J.; Cremades, E.; Barragán, F.; Alvarez, S. Covalent Radii Revisited. *Dalton Trans.* **2008**, 2832-2838.
21. (a) Lidner, E.; Auch, K.; Hiller, W.; Fawzi, R. Methyl(thioxo)phosphane: Generation and Trapping Reaction with $Mn_2(CO)_{10}$. *Angew. Chem. Int. Ed.* **1984**, *23*, 320. (b) Graham, T. W.; Udachin, K. A.; Carty, A. J. Synthesis of σ-π-phosphinidene sulfide complexes $[Mn_2(CO)_n(\mu\text{-}\eta^1,\eta^2\text{-}P(NR_2)S)]$ (n = 8, 9) via direct sulfuration of electrophilic μ-phosphinidenes and photochemical transformation to a trigonal prismatic $Mn_2P_2S_2$ cluster. *Inorg. Chim. Acta* **2007**, *360*, 1376-1379.
22. Curtis, M. D.; Butler, W. M. Cluster complex formation from the sulphur-induced disproportionation of a Mo≡Mo triple bond. The structure of $[(\eta^5\text{-}C_5H_5)_3Mo_3(CO)_6S](\eta^5\text{-}C_5H_5)Mo(CO)_3$. *J. Chem. Soc., Chem. Commun.* **1980**, 998-1000.
23. (a) Fang, Z. G.; Hor, T. S. A.; Mok, K. F.; Ng, S. C.; Liu, L. K.; Wen, Y. S. 5-Substituted 1,3,4-oxathiazol-2-ones as a sulfur source for a sulfido cluster: synthesis and molecular structure of the 48-electron equilateral triangular manganese cluster anion $[Mn_3(\mu_3\text{-}S)_2(CO)_9]^-$. *Organometallics* **1993**, *12*, 1009-1011. (b) Yao, W. R.; Guo, D. S.; Liu, Z. H.; Zhang, Q. F. Sulfur-bridged iron and manganese carbonyl clusters: synthesis, structure and nonlinear optical properties of $[(\mu\text{-}SPh)_2Fe_2(CO)_6]_2(\mu_4\text{-}S)$ and $[PPN][(\mu_3\text{-}S)_2Mn_3(CO)_9]$. *J. Mol. Struct.* **2003**, *657*, 165-175.
24. Farrugia, L. J.; Mallinson, P. R.; Stewart, B. Experimental charge density in the transition metal complex $Mn_2(CO)_{10}$: a comparative study. *Acta Crystallogr., Sect. B* **2003**, *59*, 234-247.
25. Biryukov, B. P.; Struchkov, Y. T. Crystal structure of polynuclear polymetallic carbonyls.V. π-Cyclopentadienyltricarbonylmolybdenum-manganesepentacarbonyl. *Zh. Strukt. Khim.* **1968**, *9*, 655-664.
26. Alvarez, C. M.; Alvarez, M. A.; García, M. E.; González, R.; Ramos, A.; Ruiz, M. A. Synthesis and Decarbonylation Reactions of the Triiron Phosphinidene Complex $[Fe_3Cp_3(\mu\text{-}H)(\mu_3\text{-}PPh)(CO)_4]$: Easy Cleavage and Formation of P–H and Fe–Fe Bonds. *Inorg. Chem.* **2011**, *50*, 10937-10948, and references therein.
27. Armarego, W. L. F.; Chai, C. *Purification of Laboratory Chemicals, 7th ed.*; Butterworth-Heinemann: Oxford, U. K, 2012.
28. *CrysAlis Pro*; Oxford Diffraction Limited, Ltd.: Oxford, U. K., 2006.
29. Farrugia, L. J. WinGX suite for small-molecule single-crystal crystallography. *J. Appl. Crystallogr.* **1999**, *32*, 837-838.

30. (a) Sheldrick, G. M. A short history of SHELX. *Acta Crystallogr., Sect. A* **2008**, *64*, 112-122. (b) Sheldrick, G. M. Crystal structure refinement with SHELXL. *Acta Crystallogr., Sect. C* **2015**, *71*, 5-8.
31. Frisch, M. J.; Trucks, G. W.; Schlegel, H. B.; Scuseria, G. E.; Robb, M. A.; Cheeseman, J. R.; Montgomery, Jr., J. A.; Vreven, T.; Kudin, K. N.; Burant, J. C.; Millam, J. M.; Iyengar, S. S.; Tomasi, J.; Barone, V.; Mennucci, B.; Cossi, M.; Scalmani, G.; Rega, N.; Petersson, G. A.; Nakatsuji, H.; Hada, M.; Ehara, M.; Toyota, K.; Fukuda, R.; Hasegawa, J.; Ishida, M.; Nakajima, T.; Honda, Y.; Kitao, O.; Nakai, H.; Klene, M.; Li, X.; Knox, J. E.; Hratchian, H. P.; Cross, J. B.; Bakken, V.; Adamo, C.; Jaramillo, J.; Gomperts, R.; Stratmann, R. E.; Yazyev, O.; Austin, A. J.; Cammi, R.; Pomelli, C.; Ochterski, J. W.; Ayala, P. Y.; Morokuma, K.; Voth, G. A.; Salvador, P.; Dannenberg, J. J.; Zakrzewski, V. G.; Dapprich, S.; Daniels, A. D.; Strain, M. C.; Farkas, O.; Malick, D. K.; Rabuck, A. D.; Raghavachari, K.; Foresman, J. B.; Ortiz, J. V.; Cui, Q.; Baboul, A. G.; Clifford, S.; Cioslowski, J.; Stefanov, B. B.; Liu, G.; Liashenko, A.; Piskorz, P.; Komaromi, I.; Martin, R. L.; Fox, D. J.; Keith, T.; Al-Laham, M. A.; Peng, C. Y.; Nanayakkara, A.; Challacombe, M.; Gill, P. M. W.; Johnson, B.; Chen, W.; Wong, M. W.; Gonzalez, C.; and Pople, J. A.; *Gaussian 03, Revision B.02*; Gaussian, Inc.: Wallingford, CT, 2004.
32. Becke, A. D. Density-functional thermochemistry. III. The role of exact exchange. *J. Chem. Phys.* **1993**, *98*, 5648-5652.
33. Lee, C.; Yang, W.; Parr, R. G. Development of the Colle-Salvetti correlation-energy formula into a functional of the electron density. *Phys. Rev. B* **1988**, *37*, 785-789.
34. Hay, P. J.; Wadt, W. R. Ab initio effective core potentials for molecular calculations. Potentials for potassium to gold including the outermost core orbitals. *J. Chem. Phys.* **1985**, *82*, 299-310.
35. (a) Hariharan, P. C.; Pople, J. A. Influence of polarization functions on MO hydrogenation energies. *Theor. Chim. Acta* **1973**, *28*, 213-222. (b) Petersson, G. A.; Al-Laham, M. A. A complete basis set model chemistry. II. Open-shell systems and the total energies of the first-row atoms. *J. Chem. Phys.* **1991**, *94*, 6081-6090. (c) Petersson, G. A.; Bennett, A.; Tensfeldt, T. G.; Al-Laham, M. A.; Shirley, W. A.; Mantzaris, J. A complete basis set model chemistry. I. The total energies of closed-shell atoms and hydrides of the first-row elements. *J. Chem. Phys.* **1988**, *89*, 2193-2218.
36. (a) McLean, A. D.; Chandler, G. S. Contracted Gaussian basis sets for molecular calculations. I. Second row atoms, Z=11–18. *J. Chem. Phys.* **1980**, *72*, 5639-5648. (b) Krishnan, R.; Binkley, J. S.; Seeger, R.; Pople, J. A. Self-consistent molecular

orbital methods. XX. A basis set for correlated wave functions. *J. Chem. Phys.* **1980**, *72*, 650-654.

37. Portmann, S.; Luthi, H. P. MOLEKEL: An Interactive Molecular Graphics Tool. *CHIMIA* **2000**, *54*, 766-770.
38. Lu, T.; Chen, F. Multiwfn: A multifunctional wavefunction analyzer. *J. Comput. Chem.* **2012**, *33*, 580-592.
39. Zhao, Y.; Truhlar, D. G. A new local density functional for main-group thermochemistry, transition metal bonding, thermochemical kinetics, and noncovalent interactions. *J. Chem. Phys.* **2006**, *125*, 194101-194118.
40. Chai, J.-D.; Head-Gordon, M. Long-range corrected hybrid density functionals with damped atom–atom dispersion corrections. *Phys. Chem. Chem. Phys.* **2008**, *10*, 6615-6620.

(For Table of Contents Use Only)

Table of Contents Synopsis

The photochemical reactions of the title complex with [$Mn_2(CO)_{10}$] yield, as major products, heterometallic phosphinidene derivatives displaying Mo–P–Mn connections with substantial bond multiplicity which follow from formal replacement of a $SMoCp(CO)_2$ fragment by a $Mn(CO)_4$ one, among other processes (● = C–^{t}Bu).

Graphics for Table of Contents